AAPS PharmSciTech, Vol. 12, No. 1, March 2011 (© 2011)
DOI: 10.1208/s12249-011-9598-x

Research Article

Theme: Sterile Products: Advances and Challenges in Formulation, Manufacturing, Devices and Regulatory Aspects
Guest Editors: Lavinia Lewis, Jim Agalloco, Bill Lambert, Russell Madsen, and Mark Staples

A QbD Case Study: Bayesian Prediction of Lyophilization Cycle Parameters

Linas Mockus,[1,5,6] David LeBlond,[2] Prabir K. Basu,[3] Rakhi B. Shah,[4] and Mansoor A. Khan[4]

Received 15 March 2010; accepted 7 February 2011; published online 4 March 2011

Abstract. As stipulated by ICH Q8 R2 (1), prediction of critical process parameters based on process modeling is a part of enhanced, quality by design approach to product development. In this work, we discuss a Bayesian model for the prediction of primary drying phase duration. The model is based on the premise that resistance to dry layer mass transfer is product specific, and is a function of nucleation temperature. The predicted duration of primary drying was experimentally verified on the lab scale lyophilizer. It is suggested that the model be used during scale-up activities in order to minimize trial and error and reduce costs associated with expensive large scale experiments. The proposed approach extends the work of Searles *et al.* (2) by adding a Bayesian treatment to primary drying modeling.

KEY WORDS: Bayesian; lyophilization; quality by design.

INTRODUCTION

Lyophilization is the most common method for manufacturing parenterals when aqueous solution stability is an issue. It is central to the protection of materials, which require low moisture content (less than 1%) in order to ensure stability and require a sterile and gentle preservation process. The lyophilization process consists of three phases: first, the sterile filtered solution in partially stoppered vial is frozen, then ice is sublimed to produce a cake, and finally, the product cake undergoes a desorption phase.

During the freezing phase, most of the water (the most typical solvent) separates into ice crystals throughout a matrix of glassy and/or crystalline solute. The temperature at which solution will form ice (nucleation temperature, T_n) is inherently variable in nature, as well as dependent on a number of process and formulation variables and thus introduces inter-vial heterogeneity (2) posing process control challenges in the sublimation, or primary drying, phase.

During the primary drying phase, the sublimation of ice occurs under vacuum and increased shelf temperature to provide energy for sublimation. However, if the product temperature increases to the eutectic temperature (or collapse temperature for solutes which form amorphous solids rather than crystals), gross defects occur in the product cake, making it potentially unsuitable for pharmaceutical use. Most of the lyophilization cycle time is used on primary drying, the duration of which is usually days. Assuming steady state conditions the sublimation rate can be evaluated from Ohm's law:

$$\frac{\partial m}{\partial t} = \frac{p_i - p_c}{R_p + R_s} \tag{1}$$

where $\frac{\partial m}{\partial t}$ is the mass transfer rate for the water vapor (g/h), p_i is the equilibrium vapor pressure of ice at the temperature of sublimation interface (Torr), p_c is the total chamber pressure (Torr), R_p is the resistance of the product layer to the transfer of water vapor (Torr h/g), and R_s is the resistance of the stopper. Equilibrium vapor pressure, resistance of product, and resistance of stopper are implicitly functions of time, t, while chamber pressure is typically constant during sublimation. In order not to exceed eutectic (or collapse) temperature, a balance must be maintained between the heat transfer rate to the product and removal of heat by sublimation. Heat removal, in turn, depends on the mass transfer rate of water vapor, which, in turn, depends to a great extent on the product resistance. The product resistance, R_p, for a given vial is a reflection of how the initial solution was frozen. The small size of the pores in the solute matrix previously occupied by ice crystals is the source of greatest resistance to the flow of water vapor. Larger ice crystals result in larger pores and, consequently, decreased product resistance to water vapor flow and decreased primary drying time. It was found that there is a direct relationship between the size of ice crystals and nucleation temperature: the higher the nucleation temperature, the larger the ice crystals are (2).

The findings and conclusions in this article have not been formally disseminated by the Food and Drug Administration and should not be construed to represent any agency determination or policy.

[1] Purdue University, Discovery Park, West Lafayette, Indiana, USA.
[2] Global Pharmaceutical Exploratory Statistics, Abbott Laboratories, Abbott Park, Illinois, USA.
[3] NIPTE, Inc., Rosemont, IL 60018, USA.
[4] FDA/CDER/OPS/OTR, Silver Spring, Maryland, USA.
[5] Purdue University, 480 Stadium Mall Drive, West Lafayette, IN 4907-2100, USA.
[6] To whom correspondence should be addressed. (e-mail: lmockus@purdue.edu)

The remaining unfrozen water requires desorption, or secondary drying, phase. Secondary drying temperatures are much higher than those of primary drying because the rate of water desorption from the solid is extremely slow at primary drying temperatures. However, the secondary drying may start only after the last vial from the batch is sublimed in order to maintain integrity of the product (i.e., exceeding eutectic, or collapse, temperature for vials not completely sublimed). As mentioned above, because of inter vial heterogeneity in nucleation temperature, the time lapse between the end of sublimation of the first and last vial can span several hours. Therefore, correct determination of primary drying end-point is of paramount importance to ensure quality of the product.

Traditionally, product temperature determines the end of sublimation drying, i.e., rapid rise of product temperature after the temperature sensor loses contact with ice is taken as evidence of the complete removal of ice from that container. However, the product temperature is measured by temperature sensors placed in a relatively small number of vials, and product in these vials can behave differently than the batch as a whole due to presence the external sensor. To account for this, various techniques are used. One of them is the application of delay or soak time before proceeding to secondary drying. This approach is not readily scalable from laboratory to production dryers. The technique of using a Pirani gauge (a thermal conductivity gauge) as an indicator of the primary drying end-point cannot be used in commercial dryers with formulations containing flammable solvents because of potential fire hazard. In addition, the accuracy of thermal conductivity gauges cannot be maintained throughout the entire lyophilization process. Other techniques like manometric temperature measurement (3), tunable diode laser absorption spectroscopy (4), and electronic moisture sensor (5) experimentally determine the end-point of primary drying.

The aforementioned techniques empirically account for the variability between vials. In the proposed approach, the inter-vial variability is accounted for using a predictive model. The prediction of the primary drying end-point is based on dry layer mass transfer resistance. The variation between vial drying times is mainly caused by the difference in resistance. Resistance, in turn, depends on the percentage of solids, product itself, and the nucleation temperature (6). The nucleation temperature, T_n, is an inherently random variable. By assuming a prior probability distribution on T_n we can estimate the posterior distribution of resistance across vials. Consequently, by using a heat and mass transfer model we could predict the end-point of primary drying. The approach is scalable as it is based on a first principle model.

MATERIALS AND METHODS

Sodium ethacrynate, a small molecule parenteral, was chosen as the active pharmaceutical ingredient. The commercially available drug product is a strong diuretic used to treat edema. Sodium ethacrynate was formed in aqueous solution by titration of ethacrynic acid (Sigma) with 1N sodium hydroxide solution.

The nucleation temperature and dry layer mass transfer resistance of sodium ethacrynate was estimated from the lyophilization cycle data for ten different laboratory scale batches. FTS LyoStar II lyophilizer was utilized to run the batches. Each batch consisted of 70–90 identical 10 mL glass tubing vials. Fill volume of all vials was 2.5 mL. All vials were filled with 20 mg/mL pure API solution buffered in 5 mM sodium phosphate prepared in Milli-Q Water (18 MΩ or greater). The processing conditions between batches were slightly different, i.e., loading time, ramp rate to freezing temperature, annealing temperature, and annealing time were varied. Thermocouples were placed in the center vials to mitigate "edge vial effect", i.e., radiation effects from walls and a door were shielded by neighboring vials (7). There were three to six "thermocouple" vials in each batch—total 56 vials. One of the batches was used to determine the distribution of nucleation temperature. To prevent premature nucleation induced by thermocouples inside vials, thermocouples were taped on the outside of randomly selected vials. Those thermocouples were in addition to thermocouples typically placed inside of vial to determine temperature profile during freezing, primary, and secondary drying. They were placed on randomly selected 11 vials.

DATA ANALYSIS WAS PERFORMED USING WINBUGS 1.4.3 (8) AND R 2.11.1 STATISTICAL PACKAGES

Results

Typical temperature profiles for different vials during freezing are depicted in Fig. 1. The nucleation event may start at various times and at different temperatures as indicated by the figure. Nucleation temperature, T_n, is taken as the temperature at which nucleation starts.

Typical temperature profiles for different vials during primary drying are depicted in Fig. 2. Temperature data was fitted as per methodology presented in (9) to determine the resistance. The summary of heat and mass transfer model is provided in Appendix A. Commonly used empirical relationship (10) of resistance as a function of the thickness of the sublimed powder was used:

$$\widehat{R_p} = R_0 + \frac{A_1 * l}{1 + A_2 * l} \tag{2}$$

where $\widehat{R_p} = R_p * A_p$ is the area normalized dry layer resistance (cm^2 Torr h/g), A_p is the geometric cross-sectional area of the product normal to the direction of water vapor flow (cm^2), and l is the dry layer thickness (cm). Product resistance, R_p, is implicit function of time and is calculated by solving system of differential equations, which define heat and mass transfer model, see appendix A. Dry layer thickness, l, is evaluated using Eq. 2 for the given resistance parameters R_0, A_1, A_2.

The fitting of temperature data was accomplished using ordinary least squares, i.e., resistance parameters R_0, A_1, A_2 were found by minimizing the sum of squared residuals:

$$\min \sum_{k=1}^{n} \left(T_{bt_k} - \widetilde{T_b}(R_0, A_1, A_2, t_k) \right)^2 \tag{3}$$

where T_{bt_k} is the temperature at the bottom of the vial experimentally measured at time t_k, $\widetilde{T_b}(R_0, A_1, A_2, t_k)$ is the theoretical temperature at the bottom of the vial evaluated

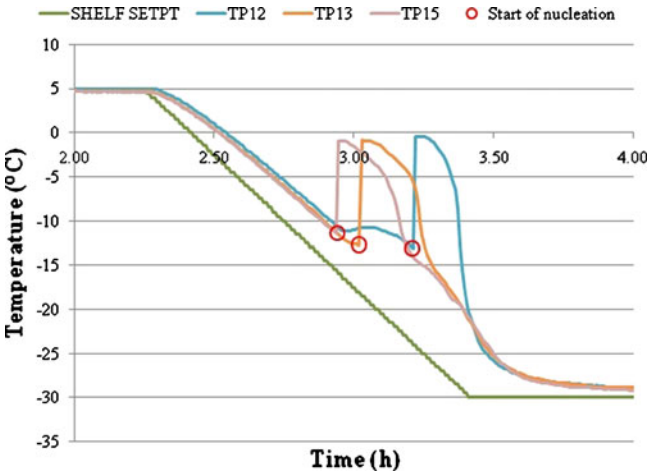

Fig. 1. Typical temperature profiles during freezing. The nucleation event occurs around 3 h after the start of the freeze–drying cycle. The nucleation event occurs when the solution is supercooled to around −10°C. It may start at different times and different temperatures as shown in the figure. After nucleation starts, the temperature rapidly rises to the equilibrium freezing temperature of water. Nucleation temperature, T_n, is determined as the temperature of solution when the nucleation starts. It is depicted as *red circle*. The *green line* represents shelf temperature set point. The remaining *lines* represent temperature profiles in different vials. The temperature is measured by a thermocouple located at the bottom inside of the vial since this is its coldest point

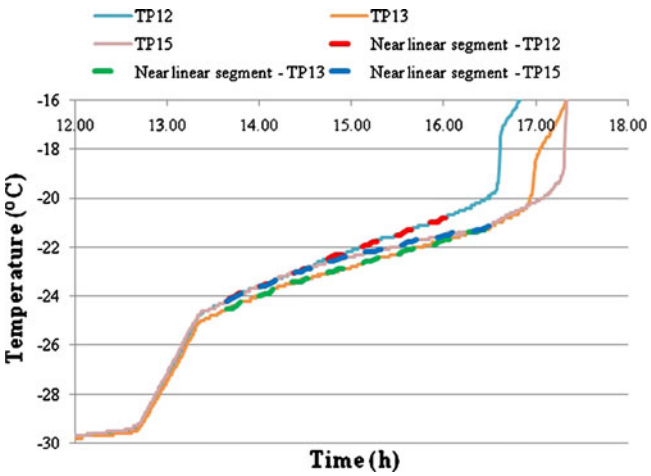

Fig. 2. Typical temperature profiles during primary drying. The sublimation of ice starts when the shelf temperature begins to rise from −30°C to 10°C. Initially, the temperature at the bottom of the vial increases almost linearly and temperature profiles in different vials are virtually superimposed. However, the temperature profiles in different vials become distinct after the shelf temperature is raised to the primary drying temperature of 10°C. The sharp rise in the temperature at the bottom of the vial indicates that sublimation in the given vial is nearly complete. The fitting is performed using the near linear segment (indicated by *dashed lines*) after shelf temperature reaches primary drying temperature and before the sublimation in given vial is complete. *Solid lines* represent temperature profiles in different vials. The temperature is measured by a thermocouple located at the bottom of the vial since this is its coldest point. Note that only the part of primary drying profile is shown (including the point when there is no ice between thermocouple and vial bottom)

from heat and mass transfer model at time t_k, n is the number of data points for a given vial, and t_k is the time of data point k. Matlab was used to perform nonlinear regression, see Eq. 3. Details of the model can be found in (9). The model incorporates conductive heat transfer from the coolant through the shelf, radiative heat transfer through the air space, and conductive heat transfer through the glass of the vial to the bottom of the ice (see Fig. 3). Heat transfer then continues through the ice from bottom to top. The top of the ice is called the interface. As sublimation proceeds, the interface moves toward the bottom of the vial, leaving a dried product layer behind. Mass transfer occurs through the dry product layer, through the stopper and chamber to condenser. The resistance to the mass transfer by the stopper and condenser is negligible compared with the dry layer mass resistance (11). A pseudo-steady state is assumed, i.e., at each point of time equilibrium is achieved.

The heat and mass transfer model is described by a system of nonlinear first-order differential equations and was solved using Matlab. Resistance for each minute during primary drying was calculated using Eq. 2 and then averaged over total sublimation time. The resistance parameters R_0, A_1, A_2 were result of fitting temperature data for each vial. The experimental data of average resistance *versus* nucleation temperature as well as linear regression function is depicted in Fig. 4. Based on this result, we propose empirical

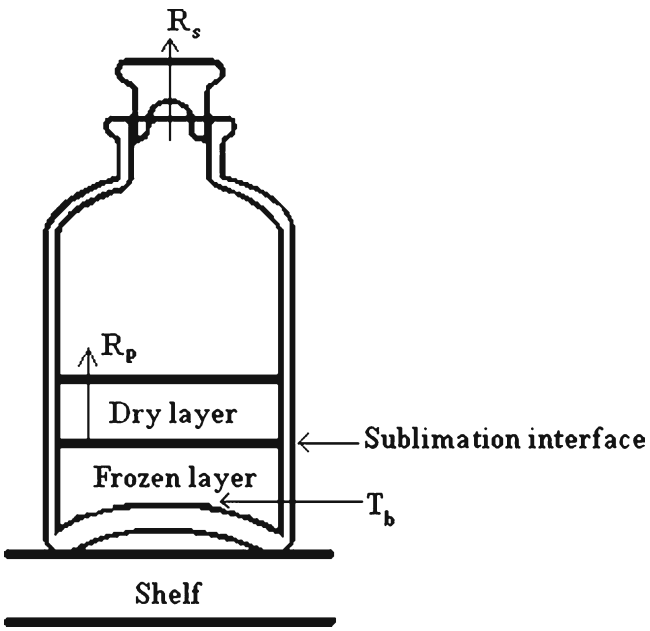

Fig. 3. Heat and mass transport during primary drying. Heat flows from the coolant through the shelf, through the air space between shelf and the bottom of the vial, and through the glass of the vial to the bottom of the ice. Heat flow then continues through the ice from bottom to top. The top of the ice is called the interface. As sublimation proceeds, the interface moves toward the bottom of the vial, leaving a dried product layer behind. Mass transfer occurs through the dry product layer, through the stopper and chamber to condenser. The resistance to the mass transfer by the stopper and condenser is negligible compared with the dry layer mass resistance. A pseudo-steady state and is assumed, i.e., at each point of time equilibrium is achieved

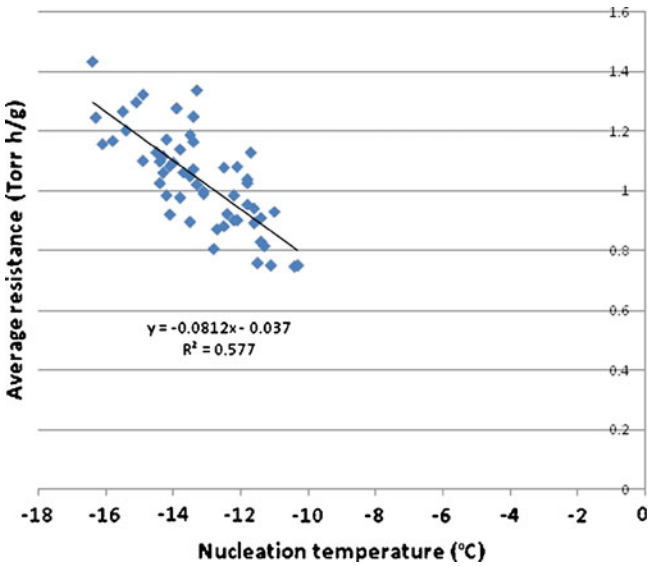

Fig. 4. Average dry layer mass transfer resistance *versus* nucleation temperature. Data is collected from batches run only on LyoStar II to prevent error introduced by shelf heat transfer coefficient. Experimental data shows that resistance decreases with a higher nucleation temperature as larger ice crystals (and consequently larger pores) are formed. Data is consistent with that reported in the literature (2). The fitted line and prediction equation with R^2 were obtained by simple linear regression

relationship between the measured nucleation temperature, T_n, and the average resistance, $\overline{R_p}$:

$$\overline{R_p} = \alpha + \beta * T_n + \varepsilon \tag{4}$$

where ε is a normal random error $\sim N(0, \sigma^2_{R_p})$.

It should be noted that an errors-in-variables model could be used in the determination of the regression function since nucleation temperature is not an error-free independent variable. However, it was determined that the advantage of using an errors-in-variables model is negligible.

Nucleation temperature may be considered a normally distributed random variable. Based on the samples from 11 vials with thermocouples taped outside, the average nucleation temperature across vials was determined to be −12.7°C with standard deviation 1.1°C. It seems reasonable to assume a normal prior distribution, with this mean and standard deviation, among vials in a batch, i.e., $\sim N\left(\mu_{T_n}, \sigma^2_{T_n}\right)$ where μ_{T_n} is the mean of nucleation temperature for the target process and the target formulation and σ_{T_n} is the corresponding standard deviation. This prior distribution of nucleation temperature is one source of uncertainty that can be incorporated into a prediction model. Another source of uncertainty that must be considered is that associated with the estimation of the slope, intercept and residual variance, $\sigma^2_{T_n}$, for the linear regression fit of data points shown in Fig. 4. This posterior uncertainty can best be assessed by using a Bayesian approach which is based on a full probability model and produces output that facilitates prediction.

A primary objective of this work is the prediction of primary drying phase duration distribution based on a physical–chemical process model, experimental data, and prior uncertainty in the underlying model parameters. Traditional statistical methods, such as maximum likelihood, can provide point and interval estimates, but cannot produce the kind of distributional estimate desired here. Such statistical approaches cannot take into account the prior uncertainties in model parameters or factors that may be known from theory or previous experiments. In complex modeling situations, traditional approaches can provide only approximate predictions and solutions may not even be available in some cases. Consequently, a Bayesian approach was employed here to fit experimental data to Eq. 4. The Bayesian approach uses Monte Carlo simulation to obtain 20,000 "draws" of α, β, and $\sigma_{Rp}{}^2$ from their joint posterior distribution. The availability of this sample of draws greatly simplifies the task of predicting the drying duration of future vials since random draws from the assumed distribution of T_n can be combined with draws from the model parameters to obtain samples from the predictive posterior of average resistance using Eq. 4. This sample can in turn be used in Eqs. 5 and 6 to obtain a sample from the predictive posterior distribution of drying duration. As such, Bayesian approach seamlessly integrates and facilitates the tasks of data analysis and prediction.

Estimation of the parameters of the linear regression fit by Gibbs sampling was performed using WinBUGS (8). Non-informative priors were assumed for the slope, intercept, and residual variance. After a burn-in of 10,000 iterations, a sample of 20,000 draws from the joint posterior distribution of the model parameters was obtained. For each of these 20,000 draws, the predicted average of area normalized dry layer resistance was calculated, using linear regression fit of the resistance and a nucleation temperature sampled from the assumed normal prior distribution with a mean of −12.7°C and standard deviation of 1.1°C. The resulting predictive posterior distribution of resistance is shown in Fig. 5. The variation in predicted resistance thus represents both the expected variation in nucleation temperature as well as uncertainty in the linear regression fit.

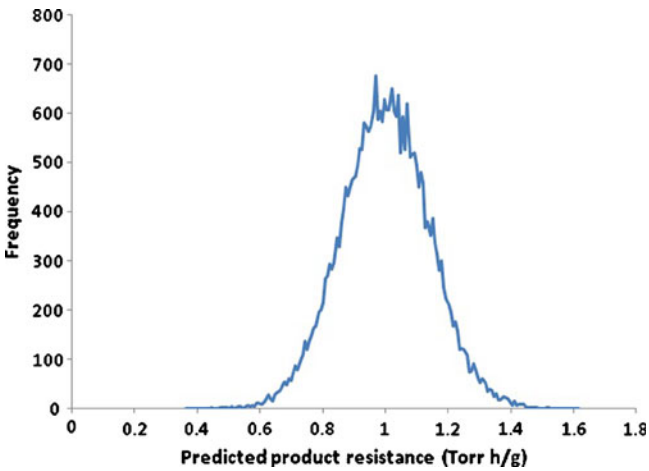

Fig. 5. Predictive posterior of average product resistance. Non-informative priors were assumed for the slope, intercept and residual variance. After a burn-in of 10,000 iterations, a sample of 20,000 draws from the joint posterior distribution of the model parameters was obtained. For each of these 20,000 draws, the predicted average of area normalized dry layer resistance was calculated, using linear regression fit of the resistance and a nucleation temperature sampled from the assumed normal prior distribution with a mean of −12.7°C and standard deviation of 1.1°C. The variation in predicted resistance represents both the expected variation in nucleation temperature as well as uncertainty in the linear regression fit

The distribution reflects information provided primarily by the observed data since the slope, intercept, and standard deviation parameters were given non-informative priors for this simulation. However, it is possible to specify informative distributions on those parameters and, most likely, the calculated distribution of resistance will change.

DISCUSSION

For verification purposes, predicted data was compared with experimentally determined primary drying durations. Duration was determined as mass of the frozen solution divided by average sublimation rate:

$$\Delta_{pr} = \frac{m_0}{\overline{\partial m/\partial t}} \tag{5}$$

where, Δ_{pr} is the primary drying duration, m_0 is the mass of the frozen solution, and $\overline{\partial m/\partial t}$ is the average sublimation rate. For the selected API, the average sublimation rate could be estimated with less than 1% of error via the following equation:

$$\overline{\frac{\partial m}{\partial t}} = \frac{\overline{p_i} - p_c}{\overline{R_p} + \overline{R_s}} \tag{6}$$

The distribution of durations using the same simulation parameters (10,000 iteration burn-in followed by 20,000 iterations in the posterior sample) is depicted in Fig. 6 along with the experimental data. The determination of primary drying end-point was on the conservative side and was based on Pirani gauge. In addition, it was found that more than 99% of water was removed during primary drying. Desorption was already occurring since the shelf temperature during primary drying was maintained at 10°C and chamber pressure was 150 mTorr. As expected, even under such conservative conditions, the most of experimental data was on the right side of distribution between mean and 97.5 percentile.

As expected, most of experimental data is located between mean and 97.5 percentile of the predicted distribution of primary drying durations. The points to the right of 97.5 percentile likely represent vials in which significant desorption occurred after the product temperature become close to the shelf temperature (10°C). It should be noted that the heat and mass transfer model does not incorporate the desorption phenomena.

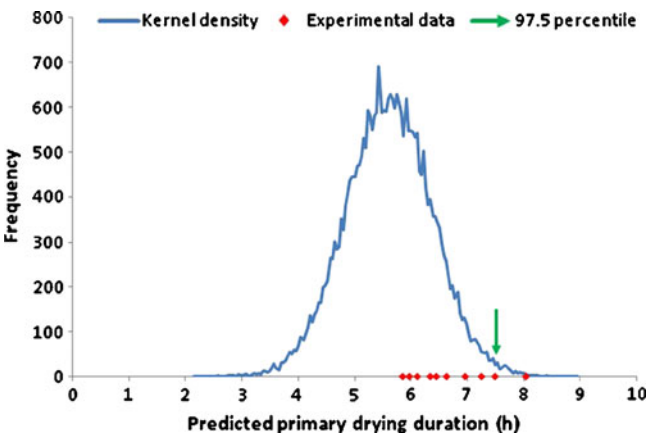

Fig. 6. Predictive posterior for primary drying duration. Experimental data is shown in *red*. *Blue line* is kernel density estimate from 20,000 WinBUGS draws calculated from Eq. 5. *Green arrow* indicates 97.5 percentile

CONCLUSIONS

The proposed approach (Appendix B) is applicable as part of lyophilization cycle scale-up protocol. The necessary parameters for the heat and mass transfer model typically are readily available. For example, the shelf heat transfer coefficient for production dryer is obtained during the corresponding operational qualification. The vial heat transfer coefficient should be determined during product development. It must be noted that distribution of nucleation temperatures in production lyophilizer needs to be determined. Since class 100 environment makes nucleation temperature more homogeneous the distribution in production freeze dryer is quite different from the distribution in lab freeze dryer (12). The primary drying end-point determined via simulation will serve as starting point for the scale-up activity and will help to minimize trial and error.

Yet another application of proposed methodology would be the acceleration of primary drying by maintaining shelf temperature as high as possible (as imposed by equipment limitations such as choke flow or powder ejection imposed by formulation limitations). This is possible while mass transfer immediately takes the heat supplied to vial away (12). Once the mass transfer becomes limiting factor, the shelf temperature has to be immediately decreased so the target product temperature is below glass transition/eutectic melt temperature. This measure is necessary in order to prevent collapse/meltback caused by a sudden rise of temperature in vials, which are not completely sublimed. By using Bayesian model combined with heat and mass transfer, it is possible to predict the time when the first vial is completely sublimed and heat transfer is not a limiting factor anymore.

Nomenclature

α	the intercept determined by linear regression of product resistance data
A_p	geometric cross-sectional area of the product normal to the direction of water vapor flow (cm^2)
β	slope determined by linear regression of product resistance data
ε	normal random error in product resistance data
l	dry layer thickness (cm)
μ_{T_n}	mean of nucleation temperature for the target process and the target formulation
m_0	mass of the frozen solution (g)
$\frac{\partial m}{\partial t}$	mass transfer rate for the water vapor (g/h)
n	number of data points for a given vial
p_i	equilibrium vapor pressure of ice at sublimation interface (Torr)
p_c	total chamber pressure (Torr)
R_p	resistance of dry layer (Torr/h/g)

R_s	resistance of stopper (Torr/h/g)
$\widehat{R_p}$	area normalized dry layer resistance (cm^2 Torr h/g)
R_0, A_1, A_2	resistance parameters
σ_{T_n}	standard deviation of nucleation temperature for the target process and the target formulation
T_{bt_k}	temperature at the bottom of the vial experimentally measured at time t_k (°C)
T_n	nucleation temperature (°C)
$\widehat{T_b}(R_0, A_1, A_2, t_k)$	theoretical temperature at the bottom of the vial evaluated from heat and mass transfer model at time t_k (°C)
Δ_{pr}	primary drying duration (h)
t_k	time of data point k (h)

ACKNOWLEDGMENTS

The project was partially supported by FDA grant #HHSF223200811270P, "Study on the development of Quality by Design (QbD) and how this can be applied to the most common parenteral process".

APPENDIX A—HEAT AND MASS TRANSFER MODEL

Heat transfer through the shelf:

$$\text{ASV} \times K_s/\Delta H_s \times 3600 \times (T_f - T_s) = \partial m/\partial t$$

ASV is shelf area per vial. For vials packed as closely as possible ASV = $1.103 \times A_v$. A_v is vial area calculated based on outside diameter (cm^2), K_s is shelf heat transfer coefficient (cal/s/cm^2), ΔH_s is heat of sublimation of ice (660 cal/g), T_s is shelf temperature (K), T_f is temperature of the cooling fluid (K),

Heat transfer between shelf and vial bottom:

$$\begin{aligned} A_v \times (K_{cs} + K_g)/\Delta H_s \times 3,600 \times (T_s - T_b) + \\ A_v \times e_s \times \sigma/\Delta H_s \times 3,600 \times ({T_s}^4 - {T_b}^4) + \\ A_v \times e_v \times \sigma/\Delta H_s \times 3,600 \times ({T_s}^4 - {T_i}^4) = \partial m/\partial t \end{aligned}$$

K_{cs} is constant associated with vial heat transfer coefficient (cal/s/cm^2/K), K_g is gas heat transfer coefficient (cal/s/cm^2/K), T_b is temperature at the bottom-center of the frozen layer (K), e_s is emissivity of the shelf surface thermal radiation, σ is Stefan–Boltzmann constant, equal to 1.35×10−12 (cal/cm^2/s/K^4), e_v is emissivity of the vial top thermal radiation, T_i is the temperature at the sublimation interface (K).

Heat transfer through the frozen layer:

$$A_p \times K_I/\Delta H_s \times 3,600 \times (T_b - T_i)/(l_{\max} - l) = \partial m/\partial t$$

A_p is cross-sectional area of the product in the vial (cm^2), K_I is effective thermal conductivity of the frozen layer (cal/s/cm/K), l_{max} is maximum thickness of the frozen layer (cm), l is thickness of dry layer (cm).

Mass transfer through dry layer:

$$(p_i - p_v)/R_p = \partial m/\partial t$$

p_i is equilibrium vapor pressure of the subliming ice (Torr), p_v is pressure in the vial (Torr), R_p is dry layer resistance (Torr h/g).

Mass transfer through stopper:

$$(p_v - p_c)/R_s = \partial m/\partial t$$

p_c is chamber pressure (Torr), R_s is stopper resistance (Torr h/g).

Clausius–Clapeyron equation to determine vapor pressure of ice at sublimation interface:

$$p_i = 2.98 \times 10^{10} \times \exp(-6,144.96/T_i)$$

Stopper resistance, see (11):

$$R_s = 1/(S_0 + S_1/2 \times (p_v + p_c))$$

S_0, S_1 are stopper mass transfer constants.

Gas heat transfer coefficient, see (11):

$$K_g = K_p \times p_c/(1 + l_v \times K_p \times p_c/\lambda_0)$$

K_p is constant associated with vial heat transfer coefficient, l_v is separation distance of the vial (cm), λ_0 is thermal conductivity of gas at ambient temperature, equal to 4.29×10−5 (cal/s/K/cm).

APPENDIX B—PROPOSED APPROACH

1. Measure nucleation temperature, T_n, during freezing, see Fig. 1. Vials should be selected randomly.
2. For these same vials, obtain temperature/time profiles during primary drying.
3. Given the particulars of the vial, stopper, solution, and lyophilizer obtain the necessary heat and transfer model parameters, i.e., vial heat transfer coefficient, vial dimensions, solids concentration, fill size, shelf heat transfer coefficient etc., based on theory or experimentally.
4. Using the primary drying profile obtained in step 2 fit the theoretical model by using Eq. 3 to obtain the resistance parameters for each vial (R_0, A_1, and A_2).
5. Based on theoretical model evaluate the product resistance, R_p, during primary drying. We found that evaluation of R_p for every minute of primary drying time is a reasonable compromise between speed and precision.
6. Calculate $\overline{R_p}$ (averaged over primary drying duration) for each vial.
7. Use a Bayesian approach to fit an appropriate predictive model (e.g., Eq. 4.) to the experimentally determined data of average resistance, $\overline{R_p}$, *versus* nucleation temperature, T_n (steps 1–6). Obtain ~20,000 draws from the posterior distribution of model parameters (i.e., α, β, and σ_{R_p}).
8. Obtain the distribution of nucleation temperature, T_n, for the target process and the target formulation. Estimate the mean $\overline{T_n}$ and standard devia-

tion σ_{T_n} , and assume a normal distribution (if appropriate).

9. Obtain estimate of average vapor pressure of ice at sublimation interface, $\overline{p_i}$, using theoretical heat and mass transfer model or experimentally. Predict the posterior duration of primary drying as described in Figures 5 and 6.
10. Use the upper percentile of the distribution obtained to estimate primary drying end-point for the target process and the target formulation.

REFERENCES

1. ICH. ICH harmonised tripartite guideline, pharmaceutical development: Q8(R2). 2009.
2. Searles JA, Carpenter JF, Randolph TW. The ice nucleation temperature determines the primary drying rate of lyophilization for samples frozen on a temperature-controlled shelf. J Pharm Sci. 2001;90(7):860–71.
3. Tang X. Evaluation of manometric temperature measurement, a process analytical technology tool for freeze-drying: part I, product temperature measurement. AAPS PharmSciTech. 2006;7(1):E1–9.
4. Nail SL, Searles JA. Elements of quality by design in development and scale-up of freeze-dried parenterals. BioPharm Int. 2008;21(1):44–52.
5. Roy ML, Pikal MJ. Process control in freeze drying: determination of the end point of sublimation drying by an electronic moisture sensor. J Parenter Sci Technol. 1989;43(2):60–6.
6. Rambhatla S, Ramot R, Bhugra C, Pikal MJ. Heat and mass transfer scale-up issues during freeze drying: II. Control and characterization of the degree of supercooling. AAPS PharmSciTech. 2004;5(4):54–62.
7. Rambhatla S, Pikal MJ. Heat and mass transfer scale-up issues during freeze-drying, I: atypical radiation and the edge vial effect. PharmSciTech. 2003;4(2):1–10.
8. Cowles M. Review of WinBUGS 1.4. Am Stat. 2004;58(4):330–6.
9. Kuu WY, Hardwick LM, Akers MJ. Rapid determination of dry layer mass transfer resistance for various pharmaceutical formulations during primary drying using product temperature profiles. Int J Pharm. 2006;313(1–2):99–113.
10. Pikal MJ, Shah S, Senior D, Lang JE. Physical chemistry of freeze-drying: measurement of sublimation rates for frozen aqueous solutions by a microbalance technique. J Pharm Science. 1983;72(6):635–50.
11. Pikal MJ. Use of laboratory data in freeze drying process design: heat and mass transfer coefficients and the computer simulation of freeze drying. J Parenter Scie Technol. 1985;39(3):115–39.
12. Pikal MJ. Freeze Drying. In Swarbrick J, Boylan JC (eds) Encyclopedia of Pharmaceutical Technology.: Marcel Dekker, Inc.; 2002. 1299–1326.